Neurobiology of Aging 82 (2019) 120–127

Contents lists available at ScienceDirect

Neurobiology of Aging

journal homepage: www.elsevier.com/locate/neuaging

Normal Aging

Reduced cognitive performance in aged rats correlates with increased excitation/inhibition ratio in the dentate gyrus in response to lateral entorhinal input

Trinh Tran [a,1], Michelle Bridi [a,1], Ming Teng Koh [b], Michela Gallagher [b,*], Alfredo Kirkwood [a,b,**,1]

[a] Mind/Brain Institute and Department of Neurosciences, MD, USA
[b] Department of Psychological and Brain Sciences, Johns Hopkins University, Baltimore, MD, USA

ARTICLE INFO

Article history:
Received 3 April 2019
Received in revised form 16 July 2019
Accepted 16 July 2019
Available online 23 July 2019

Keywords:
Granule cells
Disynaptic inhibition
Lateral entorhinal cortex
E/I balance
Excitation/inhibition balance

ABSTRACT

Aging often impairs cognitive functions associated with the medial temporal lobe (MTL). Anatomical studies identified the layer II pyramidal cells of the lateral entorhinal cortex (LEC) as one of the most vulnerable elements within the MTL. These cells provide a major excitatory input to the dentate gyrus hippocampal subfield through synapses onto granule cells and onto local inhibitory interneurons, and a fraction of these contacts are lost in aged individuals with impaired learning. Using optogenetics, we evaluated the functional status of the remaining inputs in an outbred rat model of aging that distinguishes between learning-impaired and learning-unimpaired individuals. We found that aging affects the presynaptic and postsynaptic strength of the LEC inputs onto granule cells. However, the magnitude of these changes was similar in impaired and unimpaired rats. In contrast, the recruitment of inhibition by LEC activation was selectively reduced in the aged impaired subjects. These findings are consistent with the notion that the preservation of an adequate balance of excitation and inhibition is crucial to maintaining proficient memory performance during aging.

1. Introduction

Aging often has a negative impact on cognitive abilities, particularly on learning and the encoding of new memories. It was early recognized that these impairments occur in the absence of significant neuronal loss but are more likely due to alterations in the strength, connectivity, and plasticity of circuits within the medial temporal lobe (MTL) (Gallagher et al., 2006; Rapp and Gallagher, 1996), which comprises the hippocampal formation and medial temporal cortex (entorhinal, perirhinal, and parahippocampal regions). Within the MTL memory system, proficient episodic memory critically depends on the computational properties of the dentate gyrus (DG) that receives highly processed input from layer II neurons of the entorhinal cortex (EC). This pathway provides excitatory input to both excitatory granule cells (GCs) and inhibitory interneurons in the DG. Information processing in the DG performs pattern separation, referring to the highly distinctive encoding of input in a sparse network of GCs (Leutgeb et al., 2007; McHugh et al., 2007; Neunuebel and Knierim, 2014). Such encoding is crucial to minimize interference between representations of similar but not identical experiences in episodic memory.

Recent studies have revealed that in elderly humans, memory loss and mild cognitive impairment correlate with reduced structural connectivity between the entorhinal cortex and the DG (Scheff et al., 2006; Yassa et al., 2010a,b), a diminished capacity for pattern separation in tests of memory performance, and hyperactivity in the dentate/CA3 subfields of the hippocampus (for review see Leal and Yassa, 2015). Indeed, hyperactivity appears to be a dysfunctional condition common to cognitive impairment in aged rodents (Wilson et al., 2005a, b), mouse models of Alzheimer's disease (AD) (Palop et al., 2007), and elderly humans diagnosed with mild cognitive impairment (Bakker et al., 2012; Yassa et al., 2011) potentially contributing to a reduced capacity for pattern separation in the DG.

Although much evidence has indicated a reduction in the layer II input to the DG in aging based on studies in both laboratory animals

* Corresponding author at: Department of Psychological and Brain Sciences, 216B Ames Hall 3400 N. Charles St, Baltimore, MD 21218, USA. Tel.: +410-516-0167; fax: +410-516-6205.
** Corresponding author at: Mind Brain Institute, Johns Hopkins University, 250 Dunning Hall 3400 N. Charles St, Baltimore, MD 21218, USA. Tel.: +410-516-6410; fax: +410-516-8648.
E-mail addresses: michela@jhu.edu (M. Gallagher), kirkwood@jhu.edu (A. Kirkwood).
[1] These authors contributed equally.

0197-4580/$ – see front matter © 2019 Elsevier Inc. All rights reserved.
https://doi.org/10.1016/j.neurobiolaging.2019.07.010

and humans (Bondareff and Geinisman, 1976; Rapp et al., 1999; Smith et al., 2000; Yassa et al., 2010a,b), few studies have examined the functional properties of the remaining circuitry in aging (but see Foster et al., 1991). Here, we focus on the input to the DG from the lateral EC (LEC) that innervates GC dendrites in the outer molecular layer of the DG and provides feedforward inhibition via interneurons in the DG. Anatomical and structural studies in aged rats and humans indicate that the layer II pyramidal cells in the LEC are specifically affected in memory-impaired individuals (Stranahan and Mattson, 2010; Stranahan et al., 2010, 2011), and age-related effects on this input are augmented in both prodromal and early dementia phases of late-onset AD when spreading of tau pathology initially localized in the LEC occurs (Khan et al., 2014; Kulason et al., 2019; Scheff et al., 2006; Tward et al., 2018).

Motivated by the considerations mentioned previously, we set out to evaluate how age affects the strength of synaptic excitation and synaptic inhibition in response to stimulation of LEC→GC inputs. The study was performed in a model of behaviorally characterized outbred aged rats that distinguish between impaired and unimpaired individuals (Gallagher et al., 1993; Gallagher et al., 2015). The selective activation of LEC inputs was achieved with optogenetics. We found that aging affected both presynaptic and postsynaptic function of the direct LEC excitatory inputs onto GCs, but to a similar extent in behaviorally impaired and unimpaired aged individuals. In contrast, the recruitment of disynaptic inhibition by LEC activation was selectively reduced in the aged impaired subjects. This finding is consistent with the notion that the preservation of an adequate balance of excitation and inhibition to control sparse encoding in the DG is crucial to maintaining proficient memory performance during aging.

2. Methods

2.1. Behavioral assessment

Male Long-Evans outbred rats obtained pathogen-free from Charles River Laboratories (Raleigh, NC) were 6 months (young) or 24 months (aged) of age at the time of behavioral characterization for spatial learning in a water maze (1.83 m diameter, opaque water at 27 °C). During an 8-day period, in sessions consisting of 3 trials a day with a 60-second intertrial interval, rats were trained to locate a camouflaged platform that remained in the same location 2 cm below the water surface. During a training trial, each rat was placed in the water at the perimeter of the pool and allowed 90 seconds to locate the escape platform. If within 90 seconds the rat failed to escape on a trial, it was placed onto the platform and allowed to remain there for 30 seconds. The position of entry for the animal was varied at each trial. Every sixth trial consisted of a probe trial (with the platform removed), which served to assess the development of a spatially localized search for the escape platform. During probe trials, the rat was allowed to swim a total of 30 seconds with the escape platform retracted to the bottom of the pool. After 30 seconds, the platform was raised, so that the rat could complete escape on the trial. A "behavioral index," which was generated from the proximity of the rat to the escape platform during probe trial performance, was used in correlational analysis with the neurobiological data. This index is the sum of weighted proximity scores measured during probe trials; low scores reflect search near the escape platform, whereas high scores reflect search farther away from the target. Thus, the "behavioral index" provides a measure that is based on search accuracy independent of escape velocity (Gallagher, 1993). "Search error" during training trials refers to the deviation from a direct path to the platform and provided an additional measure for behavioral analysis (Gallagher et al., 1993). Cue training (visible escape platform; 6 trials) occurred on the last day of training to test for sensorimotor and motivational factors independent of spatial learning. Rats that failed to meet a cue criterion of locating the visible platform within an average of 20 seconds over 6 trials were excluded from the experiments.

2.2. Viral transfection

Rats were anesthetized with isoflurane mixed with O_2 and transcranially injected unilaterally with 0.5 μL adeno-associated virus containing channelrhodopsin-2 (ChR2) and yellow fluorescence protein as a marker (AAV2/9.hSynapsin.hChR2(H134R)-EYFP.WPRE.hGH, Addgene26973; Penn Vector Core) into the LEC at the following coordinates: (1) bregma −5.2 mm, lateral ±7.0 mm, depth −9.0 and (2) bregma −6.3 mm, lateral ±6.0 mm, depth −8.0 mm. Rats recovered on a heated surface and were returned to the animal colony, where they remained for 6–7 weeks allowing optimal ChR2 expression.

2.3. Brain slices

All electrophysiological studies were performed by experimenters who were blind to the behavioral score of the subject. Behaviorally characterized young (6 months) and aged (24 months) rats were deeply anesthetized with isoflurane followed by urethane anesthesia (1 g/kg, i.p.) and perfused transcardially with cold dissection buffer (75 mL at 25 mL/min) containing the following (in mM): 92 N-methyl-D-glucamine, 2.5 KCl, 1.25 NaH_2PO_4, 30 $NaHCO_3$, 20 HEPES, 25 glucose, 2 thiourea, 5 Na-ascorbate, 3 Na-pyruvate, 0.5 $CaCl_2$, and 10 $MgSO_4$, pH adjusted to 7.4 with HCl. Rats were then decapitated, and the brains were removed quickly. Coronal hippocampal slices (300 μM) were prepared as described by Boric et al. (2008) in ice-cold dissection buffer bubbled with a mixture of 5% CO_2 and 95% O_2. Slices were incubated for 15 minutes at 30 °C in dissection buffer then allowed to recover for 1 hour at room temperature in artificial cerebrospinal fluid containing the following (mM): 124 NaCl, 5 KCl, 1.25 NaH_2PO_4, 26 $NaHCO_3$, 10 dextrose, 1.5 $MgCl_2$, and 2.5 $CaCl_2$, bubbled with 95% O_2/5% CO_2. All procedures were approved by the Institutional Animal Care and Use Committee at Johns Hopkins University.

2.4. Visualized whole-cell voltage-clamp recordings

All recordings were done in a submerged recording chamber superfused with artificial cerebrospinal fluid (30 ± 0.5 °C, 2 mL/min) in the presence of 100 μM 2-amino-5-phosphonovaleric acid. In some experiments 5 mM $SrCl_2$ and 10 μM bicuculline methiodide were also added. Visualized whole-cell voltage-clamp recordings were done in DG GCs with glass pipettes (4–6MΩ) filled with intracellular solution containing the following (in mM): 120 CsCl, 8 NaCl, 10 HEPES, 2 EGTA, 5 QX-314, 0.5 Na_2GTP, 4 MgATP, and 10 Na_2-phosphocreatine, pH adjusted to 7.25 with KOH, 280–290 mOsm. Membrane currents were recorded at −70 mV in the presence 100 μM 2-amino-5-phosphonovaleric acid. Cells with series resistance > 25 MΩ, input resistance < 100 MΩ, and/or root mean square noise > 4 pA were excluded from analysis. Membrane resistance and series resistance were monitored with 100-ms negative voltage commands (−4 mV) delivered before the stimulation. Cells were also excluded if series resistance changed >15% over the course of the experiment. Data were filtered at 2 kHz and digitized at 10 kHz using Igor Pro (WaveMetrics Inc, Lake Oswego, OR). All drugs were purchased from Sigma or R&D (Tocris).

Excitatory events were evoked by LED flash (520 nm, 3 ms whole field through the objective using Thorlabs parts) and quantified as described before (Petrus et al., 2014). In the presence of Sr^{+2}, which promotes asynchronous release, the average quantal size (the

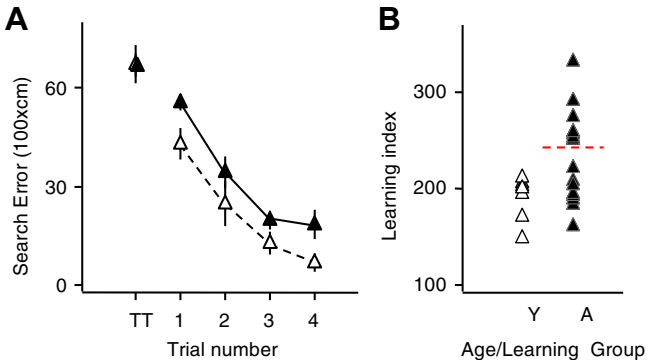

Fig. 1. Behavioral characterization of young and aged rats in the spatial version of the Morris water maze. (A) Cumulative search error measure of learning in 5 trial blocks during water maze training. This measure reflects the distance of the rat from the escape platform throughout its search, with higher numbers indicating worse performance. On the initial training trial (TT), there was no difference in the performance of young and aged rats. Statistical analysis described in the text indicated that the aged rats overall performed more poorly than young over the course of training. Data points represent the average for blocks of 5 training trials ± SEM. (B) A learning index measure for each rat was derived from proximity of the rat's search during probe trials interpolated throughout training as described in Gallagher et al. (1993), with lower scores indicating more accurate performance. As a group, aged rats exhibited significant impairment in accuracy and a larger variability of individual outcomes. Nearly half of the aged rats performed more poorly than young rats (designated aged impaired), whereas the rest performed within the range of younger adults (designated aged unimpaired). Abbreviations: A, aged rats; Y, young rats.

response evoked by a single vesicle) can be directly obtained from the isolated events recorded shortly after stimulation after correcting for spontaneous events occurring before the stimulation. A 400-ms window before LED was used for quantifying spontaneous events (pre-LED), and a 400-ms window following a 50-ms delay from LED onset was used for quantifying LED-evoked desynchronized events (post-LED). These trials were repeated until at least 60 post-LED events were accrued. We considered only cases in which the number of post-LED events was at least twice the number of pre-LED events. The average amplitude of the quantal events evoked (avQev) by the LED flash was computed from the frequency (F) and amplitude (A) of isolated events recorded before (spontaneous events) and after stimulation (spontaneous + desynchronized evoked events) using the formula: avQev = [(post-LED amplitude x post-LED frequency) − (pre-LED amplitude x pre-LED frequency)]/(post-LED frequency − pre-LED frequency). The rate and amplitude of the quantal events were computed using the Mini Analysis Program (Synaptosoft) as previously described (Morales et al., 2002). For event discrimination, we used an amplitude threshold of 3 times the root mean square noise and a rise time of <3 ms. The experimenter confirmed the events detected by the program.

To evaluate the E/I ratio, an internal pipette solution containing 125 mM Cs-gluconate, 8 mM KCl, 1 mM EGTA, 10 mM HEPES, 4 mM ATP, 5mM QX-314 and 0.5 mM GTP; pH 7.4; and 285–295 mOsm was used. Excitatory and inhibitory current reversal potentials were measured to be +10 mV and −55 mV, respectively, without compensating for the junction potential. Stimulation series over a range of light intensities were delivered while holding at each reversal potential to generate input-output curve for both excitatory and inhibitory postsynaptic currents (EPSC and IPSC). With higher intensities, the ratio of the EPSC and IPSC amplitudes (E/I ratio) converged to a stable value. This stable value was taken as the evoked E/I ratio in that cell.

2.5. Statistical analysis

Statistical significance was determined with Prism GraphPad using analysis of variance (ANOVA) tests followed by Tukey's multiple comparison test, when the data were distributed normally (judged by the D'Agostino-Pearson normality test), or by the Kruskal-Wallis test followed by the Dunn test. Statistical significance for post hoc tests was set at 0.05.

All procedures were approved by the IACUC at Johns Hopkins University.

3. Results

The aim of the study was to evaluate changes associated with cognitive aging in the synaptic inputs from the LEC onto the GCs in the DG. To that end, we combined optogenetics, to specifically activate LEC input, with whole-cell methods to record EPSC and IPSC. The measurements were done in slices prepared from young mature (6-month-old) and aged (24-month-old) outbred Long-Evans rats that had been behaviorally characterized in a standardized spatial learning protocol in a Morris water maze as described previously (see Section 2) and subsequently infected with an AAV-ChR2 in the LEC approximately 6 weeks before the final experiment.

Fig. 1 summarizes the behavioral assessment of the rats used in this study. Performance in the first trial (TT data point, Fig. 1A), before the rats had experienced escaping to the hidden platform in the water maze, was similar in both age groups. Over the course of training, however, young rats were more proficient in learning to locate the platform. A two-way ANOVA (Age x Trial Block) showed that performance improved over the course of training (Trial Block, $F(3,76) = 25.24$, $p = 0.001$) but yielded a significant difference in overall performance between the 2 age groups [Age, $F(1,76) = 10.94$, $p = 0.001$]. The interaction between Trial Block and Age was not significant [$F(3,76) = 0.22$, $p = 0.882$]. The learning index scores (Fig. 1B), computed from a key measure of search accuracy during interleaved probe trials, also differed according to age, with the young rats performing significantly better than the aged rats (Mann-Whitney U test = 28, $p = 0.046$). In agreement with previous research in this model, the aged rats displayed a range of outcomes, with a subset of aged rats performing on par with young adults and a substantial subset performing outside the range of young performance. Aged rats performing outside the range of the young group were designated as aged impaired (AI), whereas those performing on par with young adults (Y) were designated as aged unimpaired (AU). The cutoff used to identify AI and AU subgroups in the present study was consistent with normative data in this research population collected over many years.

3.1. Age-related changes in response to input from LEC onto DG do not distinguish between AU and AI rats

The comparison of the strength of LEC→GC inputs between individuals using optogenetics in slices is limited by variations in the number of axons recruited, which in turn depends on contingencies such as the extent of the viral transfection, the expression of ChR2, and the slice sectioning. Therefore, we focused the analysis on the quantification of intrinsic determinants of synaptic transmission, such as the quantal size of the postsynaptic response to the release of a single neurotransmitter vesicle. To that end, we used the divalent cation strontium (Sr^{2+}) desynchronization approach that promotes the asynchronous release of neurotransmitters and allows individual quantal events (caused by the release of a single vesicle) to be resolved and quantified (asterisks in Fig. 2B). Although it is not possible to determine whether a given isolated event is spontaneous or evoked, the average quantal size of the evoked responses in a given cell can be computed from the frequency and amplitude of isolated events recorded before (spontaneous events) and after stimulation (spontaneous + desynchronized evoked events. See Fig. 2B and Section 2 for more details). The results,

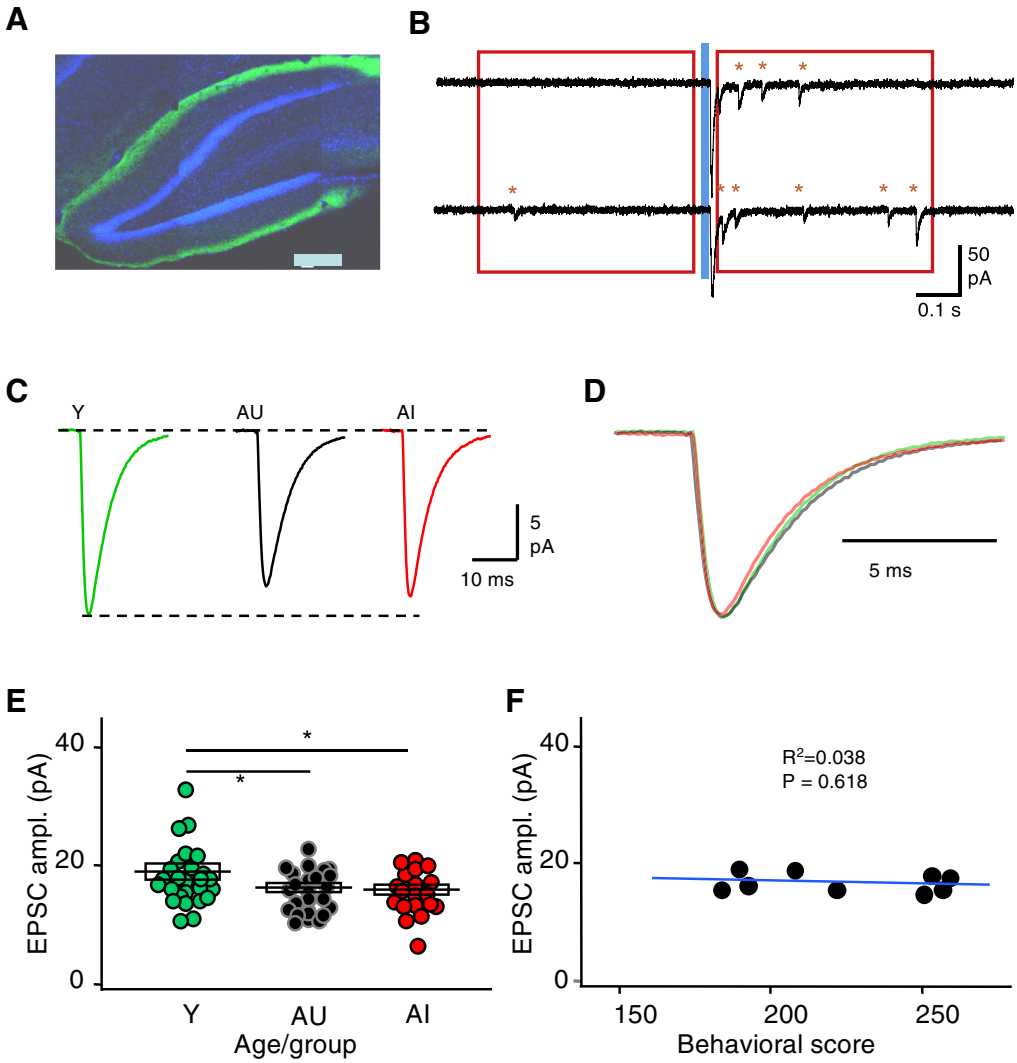

Fig. 2. Aging reduces the postsynaptic strength of the inputs from the lateral entorhinal cortex onto granule cells. (A) Example of YFP-expressing inputs (shown in green) in the DG of a rat injected with AAV-ChR2-EYFP in the lateral entorhinal cortex, Granule cells were stained with DAPI (shown in blue; calibration: 300 μm). (B) Current traces are examples of optogenetically evoked (blue line) LEC→GC synaptic responses exhibiting Sr^{+2}-induced desynchronization. Red boxes indicate the time windows used to detect isolated synaptic events (red asterisks) before and after stimulation. (C) Traces represent the computed quantal response for LEC→GC averaged across all cells recorded in each of the 3 groups. The amplitude was larger in the young group (Y: green trace) than in the aged unimpaired (AU: black trace) or in the aged impaired (AI: red trace) groups. (D) The superimposed traces are the same one as in (C) but normalized to illustrate the similar kinetics. (E) Quantal size amplitude of the LEC→GC mEPSCs for cells in the different age groups. Color code as in (C). Boxes indicate group average ± SEM. Asterisk denotes $p < 0.05$. (F) In aged rats, the average quantal size amplitude does not correlate with behavioral score. The graph plots the mEPSC amplitude averaged by rat against the individual's behavioral score. The blue line represents the best linear fit of the data. Abbreviations: DG, dentate gyrus; EPSC, excitatory postsynaptic current; GC, granule cell; LEC, lateral entorhinal cortex; mEPSC, miniature excitatory postsynaptic current. (For interpretation of the references to color in this figure legend, the reader is referred to the Web version of this article.)

shown in Fig. 2, indicate that age does not affect the shape of the quantal events evoked in GCs. The computed events averaged across all cells in each of the 3 groups (Y, AU, and AI) superimpose proportionally when normalized for the peak amplitude (Fig. 2D), and no significant differences were detected in the rise and decay times (see Table 1 for data and statistical analysis). The amplitude, on the other hand, was affected by age (Fig. 2C and E). Compared with the young group (18.18 ± 0.96 pA), the average amplitude was

Table 1
Parameters of LEC-evoked quantal synaptic events

	N rats/cells	Amplitude (pA)	Rise time (msec)	Decay tau (msec)	RMS (pA)	R input (MΩ)	R access (MΩ)
Y	7/26	18.18 ± 0.96	1.21 ± 0.07	5.27 ± 0.19	1.78 ± 0.03	415 ± 28	19.4 ± 0.9
AU	7/27	15.49 ± 0.66	1.36 ± 0.07	5.45 ± 0.11	1.81 ± 0.03	571 ± 41	20.9 ± 0.9
AI	7/23	15.47 ± 0.80	1.45 ± 0.15	5.08 ± 0.21	1.80 ± 0.03	556 ± 35	21.7 ± 0.7
Prob.		$p = 0.0262$	$p = 0.3185$	$p = 0.1572$	$p = 0.9793$	$p = 0.0049$	$p = 0.0531$
Stats.		F (2,72)	KW	KW	KW	KW	KW
		3.833	2.29	3.7	0.042	10.62	5.87

Tabulated against the 3 age groups (Y, AU, and AI) are the parameters of the evoked events (amplitude, rise time, and decay) and the parameters of the recording conditions (RMS, R input, and R access). The corresponding statistics is indicated in the last 2 rows.
Key: AI, aged impaired; AU, aged unimpaired; Y, young; RMS, root mean square

significantly smaller in each of the aged subgroups, with no difference between the AU (15.49 ± 0.66 pA) and AI (15.47 ± 0.80 pA) subgroups of rats (Fig. 2E; Tukey's HSD post hoc tests with α set at 0.05). The smaller amplitude in aged groups did not relate to diminished recording conditions, indeed the input resistance was larger in the aged rats (see Table 1). To further examine the difference across the spectrum of aged rat performance, we examined the relationship between the average event amplitude and the behavioral measure of performance among the aged rats. We averaged the event amplitude from all the cells recorded in a given aged individual and plotted this value against the individual's behavioral performance in the water maze. Only individuals with 3 or more cells recorded were included in this analysis. As shown in Fig. 2F, the individuals' evoked event amplitude including all aged subjects did not correlate with behavioral performance, $r^2 = 0.038$, $p = 0.618$. In sum, aging altered the event amplitude, yet in aged individuals, the average amplitude does not predict behavioral performance.

In a subsequent set of studies, we evaluated possible age-related alterations in presynaptic release using paired-pulse stimulation, which provides an approximate estimate of changes in release probability. In these experiments, synaptic responses were evoked with paired light pulses at interstimulus intervals (ISIs) of 50 ms, 100 ms, and 200 ms (Fig. 3A). The results indicate that aging altered the paired-pulse amplitude ratio (PPR: response 2/response 1) of the responses, but only those evoked with a 100-ms ISI. A two-way ANOVA confirmed the differences in time intervals ($F(2,162) = 37.55$, $p = 0.001$) among the 3 groups, $F(2,81) = 5.847$, $p = 0.004$. Although no significant interaction between group and time interval was detected, $F(4, 162) = 1.811$, $p = 0.129$, Tukey's post hoc tests (with α set at 0.05) indicated that at the 100-ms ISI, the average PPR in each of the aged groups (AU and AI) was smaller than the young group (Y), with no difference between the 2 aged subgroups. As in the case of the event amplitudes, the average value of the PPR at 100-ms ISI per rat did not correlate with the individual's behavioral score (Fig. 3C; $r^2 = 0.084$, $p = 0.447$). The smaller PPR in the aged groups is consistent with an increased presynaptic release probability, which could serve as a compensation to maintain input strength in the face of reduced postsynaptic responsiveness. In any case, it must be noted that although age affects both presynaptic and postsynaptic measures of synaptic efficacy, none of these changes distinguished AI from AU individuals.

Ca entry through ChR2 can increase the release probability in some, but not all synapses, and reduce paired-pulse facilitation (Jackman et al., 2014). Thus, it is possible that the optogenetic approach might have underestimated the actual PPR values. This, however, does not invalidate the central finding reported here that the PPR does not distinguish between AU and AI.

3.2. Increased excitation/inhibition ratio in the AI rats

The balance of synaptic excitation and inhibition is crucial for neural function in general, and for pattern separation in the DG in particular. GCs in the DG are subjected to strong feedforward inhibition recruited disynaptically by entorhinal inputs. Therefore, we asked whether age affects the ratio of synaptic excitation and inhibition (E/I ratio) evoked by optogenetic activation of LEC inputs. To that end, we recorded evoked EPSC and IPSC in the same GC by holding the membrane at the reversal potential for GABA (−55 mV) and AMPA receptors (10 mV), respectively. As illustrated in Fig. 4A, substantial disynaptic feedforward inhibition occurs after the EPSC. Because the E/I ratio varies with stimulation intensity (Hsu-Lien, 2016; Morales et al., 2002), we stimulated each cell at a range of intensities to determine the intensities over which the E/I ratio is stable (Fig. 4B). The findings indicate that age does affect the E/I ratio of the responses evoked by LEC inputs (Kruskal-Wallis = 16.77, $p = 0.001$), with a change occurring specifically in the AI group, which exhibited the largest values for the E/I ratio (AI: 0.583 ± 0.068, n = 23; AU: 0.251 ± 0.038, n = 20; Y: 0.307 ± 0.037, n = 21). Dunn's test (with α set at 0.05) confirmed the significance of the differences between AI and each of the other groups. Moreover, the E/I ratio and behavioral performance among the aged rats were significantly correlated (Fig. 4C; $r^2 = 0.601$, $p = 0.042$). These results are consistent with the notion that the integrity of inhibitory circuits is crucial for feedforward function in the DG.

4. Discussion

The current findings indicate that aging alters the properties of excitatory LEC inputs onto GCs. Some of these findings did not distinguish the cognitive characterization for individual differences among the aged rats. Indeed, such alterations appeared to be generally related to aging and are unlikely to serve as critical features accounting for individual differences in hippocampal-dependent function. On the other hand, a profile in E/I balance in response to LEC stimulation distinguished the AI rats from both Y and AU cohorts. This finding adds to other AI effects that distinguish aging with impairment from young adults and aged rats with preserved cognitive function in this model (e.g., Boric et al., 2008; Haberman et al., 2017a,b; Lee et al., 2005; Smith et al., 2000; Spiegel et al., 2013; Stranahan et al., 2010; Yang et al., 2013).

An opposing effect on presynaptic and postsynaptic strength could reflect the engagement of compensatory mechanisms to

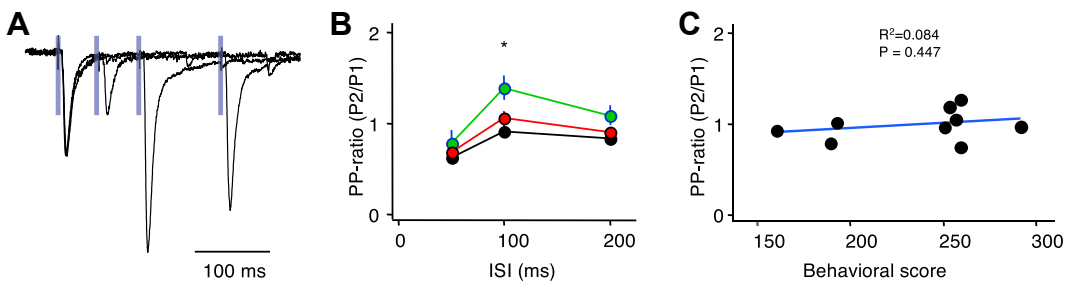

Fig. 3. Aging reduces the paired-pulse facilitation of the inputs from the lateral entorhinal cortex onto granule cells. (A) Superimposed traces are examples of optogenetically evoked responses to paired-pulse stimulation of 3 different intervals (50 ms, 100 ms, and 200 ms). Traces are normalized to the first response. Blue line indicates the 3-ms light pulse. (B) Paired-pulse response ratio (PPR = Response 2/Response 1) is increased in the young group (green) compared with the 2 aged groups (aged impaired: red; aged unimpaired: black). The asterisk denotes $p < 0.05$ (Tukey post hoc test). (C) The PPR obtained at 100-ms interval does not correlate with the individual's behavioral score. The graph plots the PPR averaged by rat against the individual's behavioral score. The blue line represents the best linear fit of the data. Abbreviations: ISI, interstimulus interval; PPR, paired-pulse ratio. (For interpretation of the references to color in this figure legend, the reader is referred to the Web version of this article.)

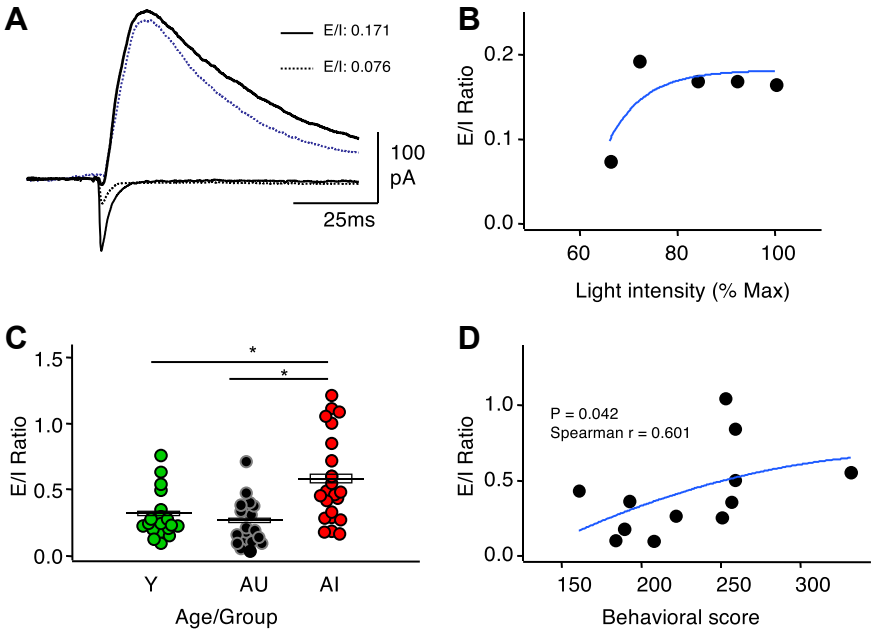

Fig. 4. Larger excitation/inhibition ratio of the LEC→GC inputs in aged impaired rats. (A) The traces are examples of excitatory synaptic responses (at a holding potential of −55 mV: lower traces) and inhibitory responses (recorded at +10 mV: upper traces) and evoked by light stimulus at lower (dotted line) and higher (solid line) intensity values. In these experiments, the excitatory/inhibitory (E/I) ratio is calculated as the ratio of the amplitudes of the excitatory and inhibitory responses. Note the different E/I ratios obtained at the 2 stimulus intensities. (B) Example showing that the E/I ratio asymptotes at increasing stimulus intensity. (C) The E/I ratio is larger in the aged impaired group than the aged unimpaired and young groups. Boxes indicate group average ± SEM. Asterisks denote $p < 0.05$. (D) The graph plots the individual's behavioral score versus the average E/I ratio of the cells recorded in that individual. The 2 variables correlate as assessed by the Spearman test. The blue lines in B and D are drawn for visual purposes. Abbreviations: DG, dentate gyrus; EPSC, excitatory postsynaptic current; GC, granule cell; IPSC, inhibitory postsynaptic current; LEC, lateral entorhinal cortex. (For interpretation of the references to color in this figure legend, the reader is referred to the Web version of this article.)

maintain overall synaptic strength. Because those synaptic changes do not correlate with differences in behavioral performance that distinguish AI and AU rats their contribution does not appear to be critical in differentiating cognitive outcomes. We believe this is a significant negative finding because changes in the amplitude of miniature synaptic responses have often been implicitly implicated in behavioral deficits observed in models of aging and neurodegenerative diseases (Chang et al., 2006; Gocel and Larson, 2013). The lack of correlation with performance in the LEC-evoked miniature events reported here suggests this is not always the case and emphasizes the importance of behavioral corroborations especially in studies of circuitry where differences have been found to be tightly associated with cognitive status.

In contrast to the absence of correlation between measures of excitatory synaptic strength of the LEC inputs and behavioral performance in the aged rats, the relative strength of synaptic inhibition recruited by LEC activation was markedly reduced in the AI rats. Reduced feedforward synaptic inhibition relative to excitation dovetails well with multiple observations of increased activation and hyperactivity in the DG/CA3 region of cognitive impaired aged individuals, both in rodents and humans (Bakker et al., 2012; Leal and Yassa, 2015; Wilson et al., 2004; Yassa et al., 2010a,b). These findings also fit with the notion that an increase in net activation could limit the capacity to support sparse coding in the DG, considered an essential condition for pattern separation in the memory encoding process.

The exact mechanisms underlying the reduced feedforward inhibition remain to be determined. The primary inhibitory neurons recruited by LEC inputs are fast-spiking parvalbumin-positive interneurons (PV-INs) (Hsu et al., 2016) and the molecular layer perforant pathway cells that target the dendrites of GC (Li et al., 2013). The fast rise time of the inhibitory response reported here (less than 5-ms rise time) is consistent with a substantial recruitment of PV-INs, providing perisomatic inhibition, which occurs faster than the molecular layer perforant pathway cells targeting distal dendrites (Li et al., 2013). An attractive and simple possibility then is that the recruitment of PV-INs by LEC inputs is reduced in the AI rats. Other scenarios are certainly plausible, for example, impaired interneuron excitability. A reduced recruitment of PV-INs, however, would be consistent with reports implicating dysfunctional PV-IN circuitry in aging and the early stages of AD in rodent models (Iaccarino et al., 2016; Kann, 2016; Verret et al., 2012) and humans (Xiao et al., 2017).

The reduced recruitment of feedforward inhibition in AI individuals complements previous reports that alterations in hilar cells providing feedback inhibition onto GC neurons are also associated with impaired performance in aging. Experimental reduction of somatostatin-positive HIPP interneurons has been demonstrated to play a critical role in DG function by limiting GC activation. With respect to the current findings, these somatostatin-positive HIPP interneurons are seemingly not recruited in a disynaptic fashion by entorhinal inputs (Hsu et al., 2016) but also undergo an age-dependent loss associated with memory impairment ((Andrews-Zwilling et al., 2012, 2010; Koh et al., 2014), including an AI selective loss in the current model of individual differences in outbred Long Evans rats (Spiegel et al., 2013). Thus, aging appears to challenge key mechanisms that contribute to the proficient encoding of episodic memory in the circuitry of the DG.

Studies of individual differences in neurocognitive aging, such as the current investigation, demonstrate that such neurobiological changes are not an invariable outcome of aging. In contrast with the individuals who are behaviorally impaired, subjects with preserved cognitive performance mainten the overall functional integrity of the LEC→GC network. Indeed, other studies using this model of neurocognitive aging have shown that AU rats have enhanced postsynaptic synaptic inhibition in GCs and enhanced tonic

inhibition in CA1 pyramidal cells (Tran et al., 2018). Moreover, preserved cognitive performance in this study population is associated with increased task-induced expression of gene markers of synaptic inhibition across hippocampal subfields in AU rats compared with young adults (Branch et al., 2019).

In sum, our analysis of the LEC inputs to GCs indicates that reduced recruitment of synaptic inhibition, rather than changes in direct synaptic excitation correlate with reduced performance in aging. Indeed, the current investigation adds to a growing body of evidence that the functionality of inhibitory circuits may bidirectionally contribute to individual differences in cognitive outcomes in aging. A loss in such function is associated with impairment while recruitment mediated via inhibitory mechanisms may contribute to resilience against functional loss in the aged brain.

Disclosure

MG is the founder of AgeneBio Incorporated, a biotechnology company that is dedicated to discovery and development of therapies, including levetiracetam, to treat cognitive impairment in aging. She has a financial interest in the company. The authors MTK and MG are inventors on Johns Hopkins University intellectual property for indication and use of levetiracetam that is licensed to AgeneBio. Otherwise, MG has had no consulting relationships with other public or private entities in the past three years and has no other financial holdings that could be perceived as constituting a potential conflict of interest. MTK has not received financial support or compensation from any individual or corporate entity for research or professional services and has no financial holdings that could be perceived as constituting a potential conflict of interest. All conflicts of interest are managed by Johns Hopkins University. All other authors have nothing to disclose.

Acknowledgements

This work was supported by the National Institute on Aging/National Institutes of Health Grants AG009973-22 to MG and AG009973-24 to AK. MB was supported by NIH T32HL110952. This study was supported by grant PO1-AG09973 from NIH.

References

Andrews-Zwilling, Y., Bien-Ly, N., Xu, Q., Li, G., Bernardo, A., Yoon, S.Y., Zwilling, D., Yan, T.X., Chen, L., Huang, Y., 2010. Apolipoprotein E4 causes age-and Tau-dependent impairment of GABAergic interneurons, leading to learning and memory deficits in mice. J. Neurosci. 30, 13707–13717.

Andrews-Zwilling, Y., Gillespie, A.K., Kravitz, A.V., Nelson, A.B., Devidze, N., Lo, I., Yoon, S.Y., Bien-Ly, N., Ring, K., Zwilling, D., Potter, G.B., 2012. Hilar GABAergic interneuron activity controls spatial learning and memory retrieval. PLoS One 7, e40555.

Bakker, A., Krauss, G.L., Albert, M.S., Speck, C.L., Jones, L.R., Stark, C.E., Yassa, M.A., Bassett, S.S., Shelton, A.L., Gallagher, M., 2012. Reduction of hippocampal hyperactivity improves cognition in amnestic mild cognitive impairment. Neuron 74, 467–474.

Bondareff, W., Geinisman, Y., 1976. Loss of synapses in the dentate gyrus of the senescent rat. Am. J. Anat. 145, 129–136.

Boric, K., Muñoz, P., Gallagher, M., Kirkwood, A., 2008. Potential adaptive function for altered long-term potentiation mechanisms in aging hippocampus. J. Neurosci. 28, 8034–8039.

Branch, A., Monasterio, A., Blair, G., Knierim, J.J., Gallagher, M., Haberman, R.P., 2019. Aged rats with preserved memory dynamically recruit hippocampal inhibition in a local/global cue mismatch environment. Neurobiol. Aging 76, 151–161.

Chang, E.H., Savage, M.J., Flood, D.G., Thomas, J.M., Levy, R.B., Mahadomrongkul, V., Shirao, T., Aoki, C., Huerta, P.T., 2006. AMPA receptor downscaling at the onset of Alzheimer's disease pathology in double knockin mice. Proc. Natl. Acad. Sci. U. S. A. 103, 3410–3415.

Foster, T.C., Barnes, C.A., Rao, G., McNaughton, B.L., 1991. Increase in perforant path quantal size in aged F-344 rats. Neurobiol. Aging 12, 441–448.

Gallagher, M., 1993. Issues in the development of models for cognitive aging across primate and nonprimate species. Neurobiol. Aging 14, 631–633.

Gallagher, M., Colantuoni, C., Eichenbaum, H., Haberman, R.P., Rapp, P.R., Tanila, H., Wilson, I.A., 2006. Individual differences in neurocognitive aging of the medial temporal lobe. Age 28, 221–233.

Gallagher, M., Burwell, R., Burchinal, M., 2015. Severity of spatial learning impairment in aging: development of a learning index for performance in the Morris water maze. Behav. Neurosci. 129, 540–548.

Gocel, J., Larson, J., 2013. Evidence for loss of synaptic AMPA receptors in anterior piriform cortex of aged mice. Front Aging Neurosci. 5, 39.

Haberman, R.P., Branch, A., Gallagher, M., 2017a. Targeting neural hyperactivity as a treatment to stem progression of late-onset Alzheimer's disease. Neurotherapeutics 14, 662–676.

Haberman, R.P., Koh, M.T., Gallagher, M., 2017b. Heightened cortical excitability in aged rodents with memory impairment. Neurobiol. Aging 54, 144–151.

Hsu, T.T., Lee, C.T., Tai, M.H., Lien, C.C., 2016. Differential recruitment of dentate gyrus interneuron types by commissural versus perforant pathways. Cereb. Cortex 26, 2715–2727.

Iaccarino, H.F., Singer, A.C., Martorell, A.J., Rudenko, A., Gao, F., Gillingham, T.Z., Mathys, H., Seo, J., Kritskiy, O., Abdurrob, F., Adaikkan, C., Canter, R.G., Rueda, R., Brown, E.N., Boyden, E.S., Tsai, L.H., 2016. Gamma frequency entrainment attenuates amyloid load and modifies microglia. Nature 540, 230–235.

Jackman, S.L., Beneduce, B.M., Drew, I.R., Regher, W.G., 2014. Achieving high-frequency optical control of synaptic transmission. J. Neurosci. 34, 13707–13717.

Kann, O., 2016. The interneuron energy hypothesis: implications for brain disease. Neurobiol. Dis. 90, 75–85.

Khan, U., Liu, L., Provenzano, F., Berman, D., Profaci, C., Sloan, R., Mayeux, R., Duff, K., Small, S., 2014. Molecular drivers and cortical spread of lateral entorhinal cortex dysfunction in preclinical Alzheimer's disease. Nat. Neurosci. 17, 304–311.

Koh, M.T., Spiegel, A.M., Gallagher, M., 2014. Age-associated changes in hippocampal-dependent cognition in D iversity O utbred mice. Hippocampus 24, 1300–1307.

Kulason, S., Tward, D.J., Brown, T., Sicat, C.S., Liu, C.F., Ratnanather, J.T., Younes, L., Bakker, A., Gallagher, M., Albert, M., Miller, M.I., 2019. Cortical thickness atrophy in the transentorhinal cortex in mild cognitive impairment. Neuroimage Clin. 21, 101617.

Lee, H.K., Min, S.S., Gallagher, M., Kirkwood, A., 2005. NMDA receptor-independent long-term depression correlates with successful aging in rats. Nat. Neurosci. 8, 1657–1659.

Leal, S.L., Yassa, M.A., 2015. Neurocognitive aging and the Hippocampus across species. Trends Neurosci. 38, 800–812.

Leutgeb, J.K., Leutgeb, S., Moser, M.B., Moser, E.I., 2007. Pattern separation in the dentate gyrus and CA3 of the hippocampus. Science 315, 961–966.

Li, Y., Stam, F.J., Aimone, J.B., Goulding, M., Callaway, E.M., Gage, F.H., 2013. Molecular layer perforant path-associated cells contribute to feed-forward inhibition in the adult dentate gyrus. Proc. Natl. Acad. Sci. U. S. A. 110, 9106–9111.

McHugh, T.J., Jones, M.W., Quinn, J.J., Balthasar, N., Coppari, R., Elmquist, J.K., Lowell, B.B., Fanselow, M.S., Wilson, M.A., Tonegawa, S., 2007. Dentate gyrus NMDA receptors mediate rapid pattern separation in the hippocampal network. Science 317, 94–99.

Morales, B., Choi, S.Y., Kirkwood, A., 2002. Dark rearing alters the development of GABAergic transmission in visual cortex. J. Neurosci. 22, 8084–8090.

Neunuebel, J.P., Knierim, J.J., 2014. CA3 retrieves coherent representations from degraded input: direct evidence for CA3 pattern completion and dentate gyrus pattern separation. Neuron 81, 416–427.

Palop, J.J., Chin, J., Roberson, E.D., Wang, J., Thwin, M.T., Bien-Ly, N., Yoo, J., Ho, K.O., Yu, G.Q., Kreitzer, A., Finkbeiner, S., Noebels, J.L., Mucke, L., 2007. Aberrant excitatory neuronal activity and compensatory remodeling of inhibitory hippocampal circuits in mouse models of Alzheimer's disease. Neuron 55, 697–711.

Petrus, E., Isaiah, A., Jones, A.P., Li, D., Wang, H., Lee, H.K., Kanold, P.O., 2014. Crossmodal induction of thalamocortical potentiation leads to enhanced information processing in the auditory cortex. Neuron 81, 664–673.

Rapp, P.R., Gallagher, M., 1996. Preserved neuron number in the hippocampus of aged rats with spatial learning deficits. Proc. Natl. Acad. Sci. U. S. A. 93, 9926–9930.

Rapp, P.R., Stack, E.C., Gallagher, M., 1999. Morphometric studies of the aged hippocampus: I. Volumetric analysis in behaviorally characterized rats. J. Comp. Neurol. 403, 459–470.

Scheff, S.W., Price, D.A., Schmitt, F.A., Mufson, E.J., 2006. Hippocampal synaptic loss in early Alzheimer's disease and mild cognitive impairment. Neurobiol. Aging 27, 1372–1384.

Smith, T.D., Adams, M.M., Gallagher, M., Morrison, J.H., Rapp, P.R., 2000. Circuit-specific alterations in hippocampal synaptophysin immunoreactivity predict spatial learning impairment in aged rats. J. Neurosci. 20, 6587–6593.

Spiegel, A.M., Koh, M.T., Vogt, N.M., Rapp, P.R., Gallagher, M., 2013. Hilar interneuron vulnerability distinguishes aged rats with memory impairment. J. Comp. Neurol. 521, 3508–3523.

Stranahan, A.M., Haberman, R.P., Gallagher, M., 2010. Cognitive decline is associated with reduced reelin expression in the entorhinal cortex of aged rats. Cereb. Cortex 21, 392–400.

Stranahan, A.M., Mattson, M.P., 2010. Selective vulnerability of neurons in layer II of the entorhinal cortex during aging and Alzheimer's disease. Neural Plast. 2010, 108190.

Stranahan, A.M., Salas-Vega, S., Jiam, N.T., Gallagher, M., 2011. Interference with reelin signaling in the lateral entorhinal cortex impairs spatial memory. Neurobiol. Learn Mem. 96, 150–155.

Tran, T., Gallagher, M., Kirkwood, A., 2018. Enhanced postsynaptic inhibitory strength in hippocampal principal cells in high-performing aged rats. Neurobiol. Aging 70, 92–101.

Tward, D.J., Sicat, C.S., Brown, T., Bakker, A., Gallagher, M., Albert, M., Miller, M., Alzheimer's Disease Neuroimaging Initiative, 2017. Entorhinal and transentorhinal atrophy in mild cognitive impairment using longitudinal diffeomorphometry. Alzheimers Dement. 9, 41–50.

Verret, L., Mann, E.O., Hang, G.B., Barth, A.M., Cobos, I., Ho, K., Devidze, N., Masliah, E., Kreitzer, A.C., Mody, I., Mucke, L., Palop, J.J., 2012. Inhibitory interneuron deficit links altered network activity and cognitive dysfunction in Alzheimer model. Cell 149, 708–721.

Wilson, I.A., Ikonen, S., Gallagher, M., Eichenbaum, H., Tanila, H., 2005b. Age-associated alterations of hippocampal place cells are subregion specific. J. Neurosci. 25, 6877–6886.

Wilson, I.A., Ikonen, S., Gureviciene, I., McMahan, R.W., Gallagher, M., Eichenbaum, H., Tanila, H., 2004. Cognitive aging and the hippocampus: how old rats represent new environments. J. Neurosci. 24, 3870–3878.

Wilson, I.A., Ikonen, S., Gurevicius, K., McMahan, R.W., Gallagher, M., Eichenbaum, H., Tanila, H., 2005a. Place cells of aged rats in two visually identical compartments. Neurobiol. Aging 26, 1099–1106.

Xiao, M.F., Xu, D., Craig, M.T., Pelkey, K.A., Chien, C.C., Shi, Y., Zhang, J., Resnick, S., Pletnikova, O., Salmon, D., Brewer, J., Edland, S., Wegiel, J., Tycko, B., Savonenko, A., Reeves, R.H., Troncoso, J.C., McBain, C.J., Galasko, D., Worley, P.F., 2017. NPTX2 and cognitive dysfunction in Alzheimer's Disease. Elife 6.

Yang, S., Megill, A., Ardiles, A.O., Ransom, S., Tran, T., Koh, M.T., Lee, H.K., Gallagher, M., Kirkwood, A., 2013. Integrity of mGluR-LTD in the associative/commissural inputs to CA3 correlates with successful aging in rats. J. Neurosci. 33, 12670–12678.

Yassa, M.A., Lacy, J.W., Stark, S.M., Albert, M.S., Gallagher, M., Stark, C.E., 2011. Pattern separation deficits associated with increased hippocampal CA3 and dentate gyrus activity in nondemented older adults. Hippocampus 21, 968–979.

Yassa, M.A., Muftuler, L.T., Stark, C.E., 2010b. Ultrahigh-resolution microstructural diffusion tensor imaging reveals perforant path degradation in aged humans in vivo. Proc. Natl. Acad. Sci. U. S. A. 107, 12687–12691.

Yassa, M.A., Stark, S.M., Bakker, A., Albert, M.S., Gallagher, M., Stark, C.E., 2010a. High-resolution structural and functional MRI of hippocampal CA3 and dentate gyrus in patients with amnestic Mild Cognitive Impairment. Neuroimage 51, 1242–1252.